

Received February 18, 2020, accepted March 29, 2020, date of publication April 10, 2020, date of current version April 30, 2020.

Digital Object Identifier 10.1109/ACCESS.2020.2987074

Analysis of Motion and Internal Loading in Redundantly Actuated Human Eyeball

JUNGKYU KIM¹, ABID IMRAN², AND BYUNG-JU YI³, (Member, IEEE)

¹Center of Human-centered Interaction for Coexistence, Seoul 02792, South Korea

²Faculty of Mechanical Engineering, Ghulam Ishaq Khan Institute of Engineering Sciences and Technology (GIKI), Swabi 23640, Pakistan

³Department of Electronic Systems Engineering, Hanyang University, Ansan 15588, South Korea

Corresponding author: Byung-Ju Yi (bj@hanyang.ac.kr)

This work was supported in part by the Technology Innovation Program (or Industrial Strategic Technology Development Program) (Development of Robotic Work Control Technology Capable of Grasping and Manipulating Various Objects in Everyday Life Environment Based on Multimodal Recognition and Using Tools) under Grant 20001856, in part by the Ministry of Trade, Industry and Energy (MOTIE, Korea), in part by the Ministry of Trade, Industry and Energy (MI, Korea), and in part by the information and communications technology (ICT)-based Medical Robotic Systems Team of Department of Electronic Systems Engineering, Hanyang University, through the Brain Korea 21 Plus Program funded by the National Research Foundation of Korea (NRF).

ABSTRACT The 3-DOF rotational motion of the human eyeball is created by using six extraocular muscles. For the force-redundant system of the human eyeball, a load distribution algorithm is proposed to investigate the dynamics and intrinsic load distribution of the eyeball. Initially, the role of each extraocular muscle is explained by describing the anatomy of the human eye. Furthermore, activity of each muscle group is analyzed to create six primitive motions of the human eye. Moreover, the dynamic model of the human eye is developed to simulate the human eye motion. Finally, a load distribution algorithm is newly developed and it is found that asymmetric arrangement of six extraocular muscles with respect to the eye axis enables the human eye not only to create the motion using minimum number of extraocular muscles, but also to ensure stability in other directions by providing antagonistic internal loading. Surprisingly, it is also found that all six primitive motions of the eyeball require three independent muscles, which is different from clinical observation so far.

INDEX TERMS Antagonistic activation, biomimetic, human eye's mechanics, redundant actuation.

I. INTRODUCTION

There exist many interdisciplinary areas, which combine biology and engineering. Understanding the behavior of the human eye requires background of both biology and engineering mechanics. The human eye is very complex organ and its movements are no exception and has special advantages like the other skeletal muscles and joints in our body. The complex mechanics and intelligent actuation system are responsible for moving the eyeballs and eyelids voluntarily and involuntarily such as quick movement of both eyes in the same direction. Furthermore, vestibule-ocular reflex movement of the eye in which the motion of the head is compensated to observe the smooth pursuit and follow the moving object [1], [2].

The mathematical modeling of biomechanical systems and body organs enhances our understanding of their behaviors and characteristics. Therefore, it is worthy of proposing an

The associate editor coordinating the review of this manuscript and approving it for publication was Rui-Jun Yan.

analytical model to understand more about the eye movement in physical ways, which will certainly benefit to promote technologies of artificial intelligence and develop more efficient vision system with superior performance like human eyes. To date, numerous efforts have been devoted to understand the human eye motion. The first mechanical model of the eye and the eyeball was developed by Ruete in 1845 [3]. Robinson [4] developed the first computerized model of the eye and its evaluation motivated many others to develop different eye models. Miller and Robinson [5] developed the most sophisticated eye model 'Orbit' which is very useful to get an overall insight into the eye mechanics problems. Furthermore, Miller [6] introduced the pulley action by adding virtual springs in model "orbit", between the muscle belly and the orbital wall [3]. All these models are lumped mechanical model.

Several other analytical models have been proposed to understand the kinematics of the human eyeball considering the geometric description of the eye movements [7], [8]. Lumped and finite element analyses (FEA) based methods

are proposed to predict the muscles activation forces for an eye movement [3], [9], [10]. Schutte *et al.* [3] proposed an FEA based method to investigate the orbital biomechanics. Karami *et al.* [9] predicted the muscle forces for eye movements by using FEA method. FEA based approaches require fewer assumptions compared to lumped models. Guo *et al.* [11] also predicted the contractile force of human extraocular muscles based on an optimization proposed herein and on the theory of mechanical equilibrium using the traditional model of eye movement. However, these approaches did not provide enough insights about redundant actuation of extraocular muscles.

On the other hand, several efforts are devoted in design and control problem of the human eye [12]–[16]. Zhang *et al.* [12] introduced a biomimetic eye robot BEBOT and performed modeling, design and analysis with accommodation mechanism. Polpitiya *et al.* [15] considered the human oculomotor system as a simple mechanical control system and analyzed the geometry and control of the human eye movement. Some robotic eye design models are proposed with reduced degree of freedom to enhance the control of the eye movement [13], [17], [18]. Luo *et al.* [18] developed an artificial eye, resembling with human to make robotic face look like human during interaction with human. Furthermore, Khan and Chen [19] proposed a multi-loop mechanism that helps to control two eyes with reduced number of actuator and less power consumption. However, in previous studies, the inherent load sharing and antagonistic internal loading are not explained in detail, which is very important to understand the primitive motions of redundantly actuated human eye system.

It is anatomically known that the human eye is controlled using six ocular muscles [20]–[22]. Academically, such system is classified as a force-redundant system. The human eye is a typical force-redundant system in that it has three rotational degrees of freedom while it is controlled by six extraocular muscles. In robotics, study on force-redundant robotic systems [23]–[30] has focused on parallel mechanisms (PM) in which there are many potential input locations. However, most of previous studies are based on symmetric structure of PM. The human eye can be also visualized as asymmetric structure of PM as will be explained in section II. Wire-driven parallel manipulator (PM) [31]–[37] has drawn much interest in the community. In such systems, at least $N + 1$ input is required to achieve N -DOF output. The biological actuator in human body (i.e., muscle) has the same characteristic however they are unidirectional. In biological system like the human body or human organs, abundant muscles are being used. Different approaches have been widely used to predict the muscles forces in musculoskeletal system during a specific motion such as prediction of muscle force in upper/lower extremities [38], face [39], and tongue [40]. However, there has not been enough study explaining the role of such abundant muscles. Based on our proposed approach, we noticed that each primitive motion of the human eye is being controlled using at least three muscles.

The main purpose of this work is to explain how the human eyeball is operated using six extraocular muscles. Considering this, the analytical methodologies are developed for force redundant system of eyeball. Specifically, to analyze the load sharing and internal loading phenomenon during eye movements. Firstly, six primitive motions of the eyeball are analyzed in terms of corresponding ocular muscle set in a qualitative way. Secondly, a novel load distribution algorithm is developed to explain the inherent muscle activation of human eyeball for each primitive motion in an analytical manner. Moreover, the motions with asymmetric arrangement of six extraocular muscles are analyzed in quantitative way. It is found that inherent arrangement of extraocular muscles is meaningful in the sense that using minimum number of muscles, both the primitive motion and internal loading can be achieved. The internal loading helps to reduce the disturbance in other motion directions.

This paper starts with anatomy of extraocular muscles in section II. Section III introduces the eyeball mechanics, explaining the relationship between the eyeball motion and six extraocular muscles. The dynamic model of eyeball and a load distribution algorithm inherent in the eyeball is proposed in section III. Simulation study to corroborate the effectiveness of the load distribution algorithm is presented in section IV. Finally, we draw conclusion.

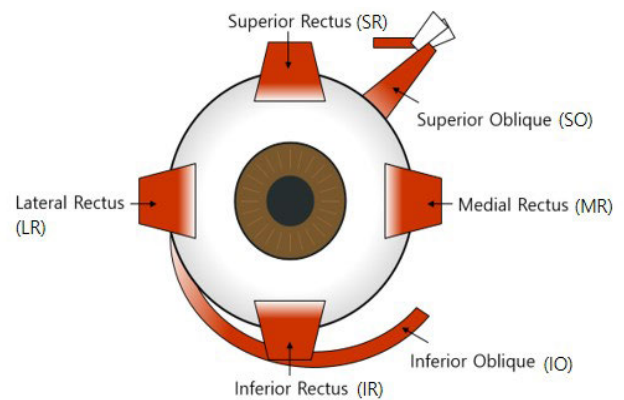


FIGURE 1. Extraocular muscles [8].

II. ANATOMY OF EXTRAOCULAR MUSCLE

A. ANALYSIS OF EXTRA-OCULAR MUSCLE

In this section, the anatomy and the function of extraocular muscles in the movement of the eyeball is explained by analyzing the motion of the human eyeball. The complete anatomy of the eye is very complex. The eyeball is surrounded by six extraocular muscles as shown in Fig. 1; Lateral Rectus Muscle (LR), Medial Rectus Muscle (MR), Superior Rectus Muscle (SR), Inferior Rectus Muscle (IR), Superior Oblique Muscle (SO), and Inferior Oblique Muscle (IO). It is interesting to note that Superior oblique muscle passes through a biological hinge, trochlea. The six extraocular muscles (EOMs) including four rectus muscles and two oblique muscles are controlled by the nerves to generate forces in each muscle. These forces rotate the eyeball to track a visual target.

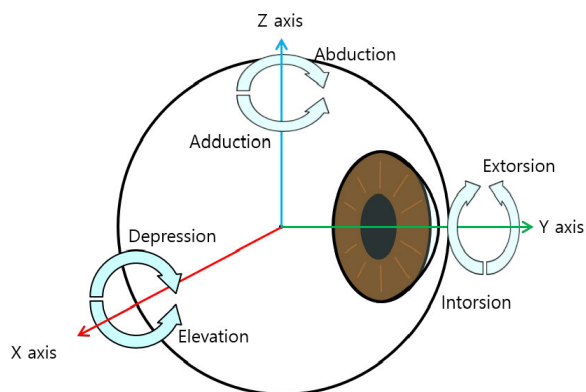


FIGURE 2. Six primitive motions of the right eye [8].

The rotational motion of the eyeball is generated through the contraction of the extraocular muscles. The eyeball performs the three DOF (degrees of freedom) movement such as roll, pitch, and yaw motion as shown in Fig. 2. The roll has an Extorsion that rotates counter clock-wisely and an Intorsion that rotates clock-wisely about Y-axis. The pitch has an upward elevation and a downward depression about X-axis. Finally, the yaw has an abduction away from the nose and adduction close to the nose about Z-axis. Accordingly, the eyeball motion is classified by those such six primitive motions.

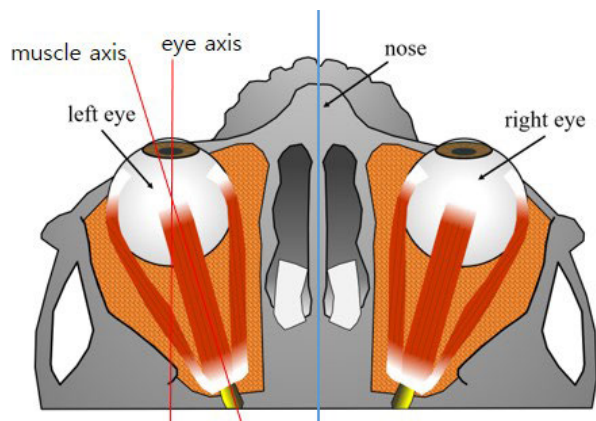


FIGURE 3. Asymmetric arrangement of extraocular muscles [8].

Anatomically, two eyeballs are arranged in a symmetric manner as shown in Fig. 3, but roots of muscles are focused to the centerline of nose. Thus, the anatomical axis are not parallel to the muscle axis and six muscles are asymmetrically arranged with respect to the anatomical axis as shown in Fig. 3. As a result, only the lateral rectus muscle and the medial rectus muscle contribute to specific motion such as Adduction and Abduction. The other four extraocular muscles contribute to secondary and tertiary auxiliary motions in addition to the main motion [20]. Table 1 summarizes the role of extraocular muscles considering the main, secondary and tertiary motions.

TABLE 1. Role of extraocular muscles [20].

Extra-ocular muscle	1 st effect	2 nd effect	3 rd effect
Medial Rectus (MR)	Adduction	-	-
Lateral Rectus (LR)	Abduction	-	-
Superior Rectus (SR)	Elevation	Intorsion	Adduction
Inferior Rectus (IR)	Depression	Extorsion	Adduction
Superior Oblique (SO)	Intorsion	Depression	Abduction
Inferior Oblique (IO)	Extorsion	Elevation	Abduction

B. MUSCLE GROUP FOR PRIMITIVE MOTIONS OF EYE

In this section, we analyze the relationship between six primitive motions of the eyeball and six muscles for the force redundant system of the human eye. Furthermore, the load sharing and antagonistic internal loading are explained during the generation of six primitive motions. Due to asymmetric arrangement of six extraocular muscles with respect to the eye axis, some combinations of muscle group are inevitable to create each primitive motion of the eyeball.

Fig. 4 describes the relationship between muscle groups and six primitive motions of the eyeball. Contribution of each muscle to the eyeball’s motion is displayed as small arrows, which denote the force or moment exerted at the center of the eyeball by each muscle. In force-redundant system, the motion is generated through load sharing and antagonistically. Forces or moments along or about the same direction imply load sharing, and forces or moments in the opposite direction imply fighting (or antagonistic internal loading).

As described in Fig. 4(a), activation of Superior rectus muscle (SR) and Inferior oblique muscle (IO) contributes to three motions of the eyeball. It is noticed that two muscles collaborate to create elevation of the eyeball as denoted by two small red arrows. However, in the other directions, forces and moments generated by two muscles, are opposite in direction as denoted by two small blue and green arrows, respectively. Due to these forces and moments, the internal loading is created in other two motion directions (i.e., along the x-direction and rotational motion about the y-axis). This, resulting antagonistic internal loading, keeps the eyeball from translation along the x-axis and rotation about the y-axes. Based on previous clinical observation [21], only two muscles are activated for Elevation, Depression, Extorsion and Intorsion motions, while three muscles are activated for Abduction and adduction motions. As illustrate in Fig 4(c), the activation of Superior rectus, Medical Rectus and Inferior rectus contributes to the three motions of the eyeball. These three muscles collaborate (load sharing) to create the Adduction motion as denoted by blue arrow. However, the antagonistic internal loading is created by two muscles in other directions as denote by green and red arrow. Which keep the

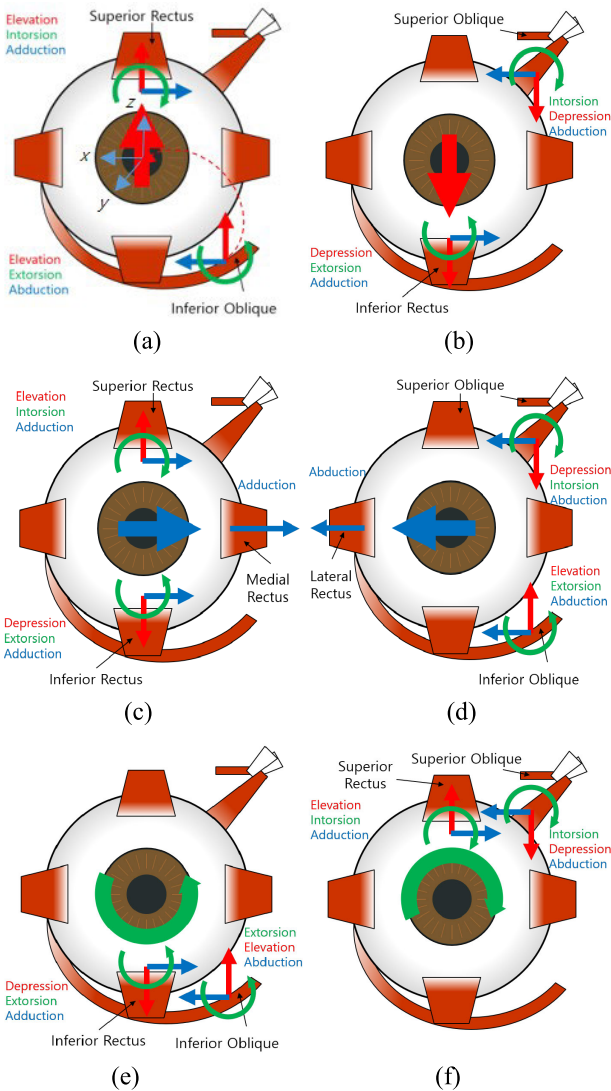


FIGURE 4. Relationship between six primitive motions and extraocular muscle groups (a) Elevation, (b) Depression, (c) Adduction, (d) Abduction, (e) Extorsion, (f) Intorsion.

eye to translate along z-direction and rotate about y-direction. Thus, it is noted that natural asymmetric arrangement of extraocular muscles with respect to the anatomical axis has certain advantages. It allows to achieve the desired primitive movement (big red arrow at the center for each primitive motion) and also provide the internal loading to resist the external disturbance exerted in other motion directions by using minimum number of muscles (Three for abduction/adduction and too for other four motions).

If the anatomical axis are parallel to the muscle axis, we need two muscles to create elevation and four muscles to create internal loading along x-direction and about y-direction. In total, six muscles are required. Therefore, asymmetric arrangement of extraocular muscles has advantage in terms of number of muscles being used.

Surprisingly, this phenomenon of load sharing and antagonistic internal loading happens in all cases as illustrated

in Fig. 4. Inspired by this phenomenon, we newly develop a load distribution algorithm to activate the corresponding extraocular muscle for each primitive motion. In Section III, mathematical detail of load distribution algorithm will be introduced.

C. CONTACT GEOMETRY BETWEEN EYEBALL AND MUSCLES

In order to describe the kinematics of the eyeball, four points should be defined in each extraocular muscle as illustrate in Fig. 5. First, each extraocular muscle has an insertion point that is attached to the eyeball and a tangential point that begins to wrap the eyeball. Furthermore, a pulley point where direction of the external ocular muscles is being changed. All extraocular muscles converge to a common origin point inside of the skull. When an extraocular muscle is activated, a tension is generated in the muscle since the origin point is fixed. And the direction of the force changes at the pulley point and finally the force is transmitted to the insertion point. Accordingly, each muscle force also creates a moment to the eyeball, which cause to rotate the eyeball about certain axis. Corresponding data of the three points for each muscle is obtained from anatomy of the human eyeball as given in Table 2.

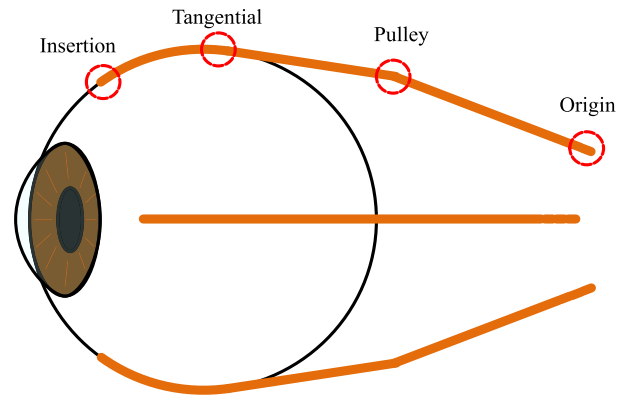


FIGURE 5. Illustration of Points of extra-ocular muscle.

III. EYE MECHANICS

In this section, the methodology is proposed to develop the eye mechanics. We made some assumptions in the development of eyeball mechanics. Which are as follows:

Assumption 1: The center of the eyeball is fixed at the origin of the eye’s Cartesian coordinate system, and it is rotated about the origin and does not move by any external force or gravity. Furthermore, there is no linear displacement in the eyeball when it is rotated by the muscles.

Assumption 2: However, the human eye is not perfect sphere, in this article the eyeball is assumed a perfect sphere whose mass is uniformly distributed. Accordingly, there is no centripetal force when the eyeball rotates. According to this assumption, the moment of inertia of eyeball is given as

follows

$$[I] = \begin{bmatrix} \frac{2}{5}MR^2 & 0 & 0 \\ 0 & \frac{2}{5}MR^2 & 0 \\ 0 & 0 & \frac{2}{5}MR^2 \end{bmatrix}. \quad (1)$$

where $[I]$ represents the moment of inertia of the eyeball. M and R denote the mass and radius of eyeball as given in table 2, respectively.

TABLE 2. Parameters of eye and extraocular muscles [21].

Eyeball Weight Eyeball Radius		7.5 gram 11.99 mm				
	Lateral Rectus	Medial Rectus	Superior Rectus	Inferior Rectus	Superior Oblique	Inferior Oblique
Origin						
x(mm)	13.00	17.00	15.00	17.00	18.00	13.00
y(mm)	34.00	30.00	31.76	31.76	31.50	10.00
z(mm)	1.00	1.00	3.60	2.40	5.00	15.46
Insertion						
x(mm)	10.08	9.65	2.76	1.76	2.90	8.00
y(mm)	6.50	8.84	6.46	6.85	8.00	9.18
z(mm)	0.00	0.00	10.25	10.22	8.82	0.00
Pulley						
x(mm)	12.00	14.00	5.16	5.16	15.27	13.00
y(mm)	8.00	5.00	10.78	8.78	11.00	10.00
z(mm)	0.33	0.14	10.00	12.00	11.75	15.46
λ Scaling factor	1.00	1.07	0.80	0.97	0.41	0.38

Assumption 3: The masses of muscles are ignored, and no force is being exerted on the eyeballs during relaxation. The friction force between muscles and eye is assumed negligible.

Assumption 4: The position of the tangential point moves as the eyeball rotates. This position is on the plane containing the origin, insertion point, and pulley point.

A. DYNAMICS MODEL OF EYEBALL

Based on the assumptions, the dynamic equation of the eyeball is described as follows

$$[I]\ddot{\theta} = \vec{T}, \quad (2)$$

where $\ddot{\theta}$ and \vec{T} denotes the angular acceleration vector of the eyeball and the torque vector created by extraocular muscles, respectively.

According to the *first assumption*, the magnitude of the tension applied to the tangential point of the eye is equal to the tension exerted by the extraocular muscle. The direction of tension is tangent to the eye contact surface at the tangential point. The tension at the pulley point is the same as that at the insertion point.

As shown in Fig. 6, the moment created by the i^{th} extraocular muscle is expressed by

$$\vec{M}_i = \vec{I}_i \times \vec{F}_i. \quad (i = 1 \cdots 6) \quad (3)$$

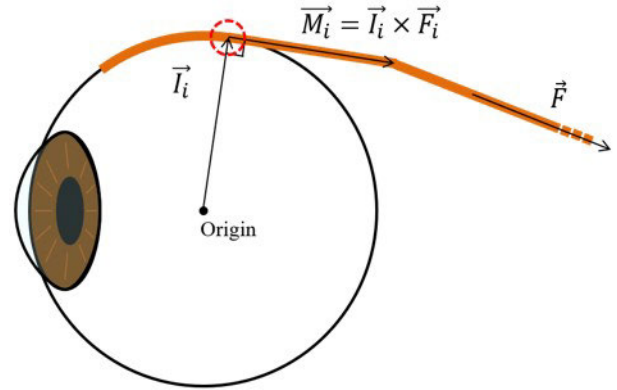


FIGURE 6. Torque created by muscle force.

where $(i = 1 \cdots 6)$ are corresponding to six muscles. Each muscle has different strength. So, when the torque of all muscle is combined, it is scaled by the proportional constant (λ_i) for each muscle. The proportional constant (λ_i) corresponding to each muscle force is given in Table 2 which is based on the clinical test [21].

Finally, the sum of all torques is described as follows

$$\vec{T}_{xyz} = \sum \vec{M}_i = \lambda_{SR} \cdot M_{SR} + \lambda_{SO} \cdot M_{SO} + \lambda_{LR} \cdot M_{LR} + \lambda_{MR} \cdot M_{MR} + \lambda_{IR} \cdot M_{IR} + \lambda_{IO} \cdot M_{IO}. \quad (4)$$

where \vec{T}_{xyz} represent the torque vector which is sum of torques generated by all muscles. The subscript in front of λ and M are corresponding to the name of each muscles such as SR for Superior rectus and so on. For simulations, the physical parameters of the eyeball, extraocular muscles points, and the tension proportional values of extraocular muscles are summarized in Table 2. This data set is for one person having normal ocular alignment, which is used in the study of Buchberger [21].

B. LOAD DISTRIBUTION ALGORITHM

In force redundant system of human eyeball, the primitive motions are created by load sharing through activation of multiple muscles. Furthermore, these muscles group provide the internal loading as well to resist the disturbance in other direction. To describe this phenomenon in analytical way, in this section we proposed a load distribution algorithm for muscle activation.

Eq. (4) can be rewritten as follows

$$\begin{aligned} \vec{T}_{xyz} &= \sum \vec{M}_i = \sum \lambda_i \vec{I}_i \times \vec{F}_i = \sum \lambda_i [R_i] e_i \|\vec{F}_i\| \\ &= [G] \vec{F}, \end{aligned} \quad (5)$$

where \vec{F} is the activation muscle force vector, $[R_i] = \vec{I}_i \times e_i = \frac{\vec{F}_i}{\|\vec{F}_i\|}$, and

$$\begin{aligned} [G] &= [\lambda_1 [R_1] e_1 \lambda_2 [R_2] e_2 \lambda_3 [R_3] e_3 \lambda_4 [R_4] e_4 \lambda_5 [R_5] e_5 \lambda_6 [R_6] e_6] \\ &\in R^{3 \times 6} \end{aligned}$$

and

$$\vec{F} = (\|\vec{F}_{SR}\| \|\vec{F}_{SO}\| \|\vec{F}_{LR}\| \|\vec{F}_{MR}\| \|\vec{F}_{IR}\| \|\vec{F}_{IO}\|)^T \in \mathbb{R}^6.$$

Finally, the general solution for muscles forces is obtained from Eq. (5) which is now given as follows

$$\vec{F} = [G]^+ \vec{T} + (I - [G]^+ [G]) \vec{e}, \quad (6)$$

where \vec{F} denotes the activation muscle force vector. And $[G]^+$ denotes the pseudo-inverse matrix of the $[G]$. The first term in Eq. (6) denotes a particular solution which minimizing the second norm of the muscle force vector and the second term denotes the homogenous solution explaining the antagonistic internal loading.

Since biological muscles are unidirectional, accordingly, the following constraints are considered while developing the load distribution algorithm

- All muscle forces should be positive value ($\vec{F} \geq 0$).
- More than two muscles should be activated to create each primitive motion. In general, the number of muscles should be greater than $N + 1$, where N is the number of outputs.

However, there is no guarantee that the particular solution of Eq. (6) yields all positive muscle forces. Accordingly, it is necessary to redistribute the muscle forces. Such algorithm can be described as follows

$$[A] \vec{F} = \vec{\alpha}, \quad (7)$$

where $[A] \in \mathbb{R}^{h \times 6}$, $\vec{\alpha} \in \mathbb{R}^h$. h implies the degrees of freedom to be used in the null space.

Finally, based on the matrix augmentation method, a load distribution algorithm is newly devolved based on the Eq. (5) and Eq. (7). Putting Eq. (5) and Eq. (7) together, we have

$$\begin{bmatrix} [G] \\ [A] \end{bmatrix} \vec{F} = \begin{pmatrix} \vec{T} \\ \vec{\alpha} \end{pmatrix}. \quad (8)$$

Finally, similar to Eq. (6) the general solution is obtained as follows

$$\vec{F} = [B]^+ \begin{pmatrix} \vec{T} \\ \vec{\alpha} \end{pmatrix} + (I - [B]^+ [B]) \vec{e}, \quad (9)$$

where $[B] = \begin{bmatrix} [G] \\ [A] \end{bmatrix}$ and the second null space denoted by $(I - [B]^+ [B])$ can be further used as long as the degrees of the null-space still remain. The working principle and generation of constraint matrix $[A]$ and $\vec{\alpha}$ is explained in section IV.

In the dynamic model given in (2), gravity, friction force and disturbance can also be included. Then, the changes in considered assumptions could affect the magnitude of the optimized/required muscles forces. However, the gravity load does not affect since the eyeball is seated on the cup surrounding the eye. Friction is considered negligible since there exists fluidic membrane between eye surface and the ocular muscles. On the other hands, uncertain disturbance to the system will affect (increase/decrease) the torque vector as given in dynamic model (2), but it is hard to model. However, even considering some uncertainty, the effectiveness and stability

of the proposed algorithm would not be affected much. Once the torque vector is computed (whatever the values of torques are), the algorithm will provide the corresponding muscle forces. The load distribution algorithm, as given in equation (9), finds the optimized muscles forces based on torque vector (\vec{T}). The effectiveness and working principle of load distribution algorithm entirely depend on the selection of matrix $[A]$ and vector $\vec{\alpha}$.

C. MUSCLE TENSILE FORCE

Since the muscles are unidirectional actuators, only the pulling tension can be applied and pushing force is hardly generated. In addition, there are two kinds of muscle tension: active tension generated by receiving electrical nerve signals and passive tension generated by changing length like a spring. The strength of these muscle tensions is dependent on the length of the muscles. Particularly passive tension occurs only when the length is increased. Hill's muscle model [41] describing the active and passive tensions according to the changed length ratio, were employed in this study.

IV. DYNAMIC SIMULATION OF EYEBALL MOTION

A. CONSTRAINT OF MUSCLE GROUP

In this section, the working principle of the proposed load distribution algorithm is elaborated. One more thing to note is that there exists a muscle group to generate each primitive motion of the eyeball as described in section II(B). Therefore, we reflect such information when redistributing the muscle forces. For instance, the Adduction (counter clockwise rotation about the z-axis) is created by only activating Medial rectus, Superior rectus, and Inferior rectus muscle as given in Table 1.

However, if we just employ the first term of Eq. (6) as solution of muscle force, all six muscle forces are calculated, which is actually not desirable. Thus, it is necessary to nullify the other three muscles forces (i.e., Superior oblique, Lateral rectus, and Inferior oblique in order). In order to achieve that, accordingly, matrix $[A]$ and $\vec{\alpha}$ in Eq. (8) are set as follows

$$[A] = \begin{bmatrix} 0 & 1 & 0 & 0 & 0 & 0 \\ 0 & 0 & 1 & 0 & 0 & 0 \\ 0 & 0 & 0 & 0 & 0 & 1 \end{bmatrix}, \quad \vec{\alpha} = \begin{pmatrix} 0 \\ 0 \\ 0 \end{pmatrix}. \quad (10)$$

As a result, through redistribution by Eq. (9), only three muscles (i.e., Superior rectus, Medial rectus, and Inferior rectus) are employed to create Adduction and the other three muscle forces are forced to have zero muscle forces. The matrix $[A]$ and $\vec{\alpha}$ are chosen to satisfy such constraints. Here, there is no more degree left in the null-space. Furthermore, the constraint conditions for six muscle groups for each primitive motion are given in Appendix.

B. DYNAMIC SIMULATION AND ANALYSIS

In this section, dynamic simulation of the eyeball is performed. The kinematic and dynamic parameters, which are used for simulation, are given in Table 2. The simulations are performed by using MATLAB. The constraint Matrix $[A]$

is constructed based on the required number of muscles and considering the ($\vec{F} \geq 0$). Then, the muscle forces are calculated based on the proposed load distribution algorithm (9) and the motions are simulated based on the dynamic model as given in (2). Lastly, the torque experienced by eyeball is calculated and, based on that torque, stable and unstable motion of eye is analyzed and required minimum number of muscles are updated. Firstly, we simulate the motion, which required the activation of three muscles such as adduction and followed by the simulation of the motion, which required the activation of two muscles such as Depression. Finally, in this section, the necessity of three independent muscles for each primitive motion will be explained by analyzing the antagonistic internal loading.

In order to simulate the eyeball motion, a trajectory of the eyeball is defined as follows.

- Give constant angular acceleration for 0.1 second to create each primitive motion of eyeball.

In order to create Adduction (i.e., counterclockwise rotation about z-axis), three muscles (MR, SR, and IR) collaborate as shown in Fig. 4(c). According to Eq. (9), three positive muscle forces to create Adduction can be calculated as shown in Fig. 7(a). Once the muscle activation forces are known, the eyeball motion is simulated by performing the numerical integration of dynamic model as given in Eq. (2). Fig. 7(b) demonstrates the result of the dynamic simulation. Which denote the incremental changes in muscle lengths during the Adduction motion. The Fig. 7(b) shows the top view of the eyeball and the motion transition of three muscles are shown as red lines.

As mentioned before, the activation of extraocular muscle group contributes to different motions of the eyeball. The activation of muscle group also results in internal loading as explained in section (B). Analytically, the second term ($(I - [B]^+ [B]) \vec{\epsilon}$) in Eq. (9) is explaining the phenomenon of the antagonistic internal loading. To analyze the existence and effect of internal forces on eyeball motion, these muscles force are analyzed in terms of torque experienced by the eyeball. Finally, the resulting torque vector, projected to the operational space of the eyeball, is expressed in the following form:

$$\begin{aligned} \vec{T} &= \vec{r}_{SR} \times \vec{F}_{SR} + \vec{r}_{MR} \times \vec{F}_{MR} + \vec{r}_{IR} \times \vec{F}_{IR} \\ &= \begin{bmatrix} \{(a_{IR})_x + (b_{MR})_x + (c_{IR})_x\} \\ \{(c_{IR})_y + (b_{MR})_y + (c_{IR})_y\} \\ \{(c_{IR})_z + (b_{MR})_z + (c_{IR})_z\} \end{bmatrix} \\ &= \begin{bmatrix} \text{moment sum @ x axis} \\ \text{moment sum @ y axis} \\ \text{moment sum @ z axis} \end{bmatrix}. \end{aligned} \tag{11}$$

Eq. (11) represents the operational space torque about each axis due to Superior rectus, Medial rectus and Inferior rectus muscles forces. In the first and second plots of Fig. 8, the summation of moment components is zero. It is confirmed that three muscle forces contribute to create antagonistic internal loading to avoid any rotational motions about x- and y-axes. Such antagonistic internal loading is beneficial to reject the

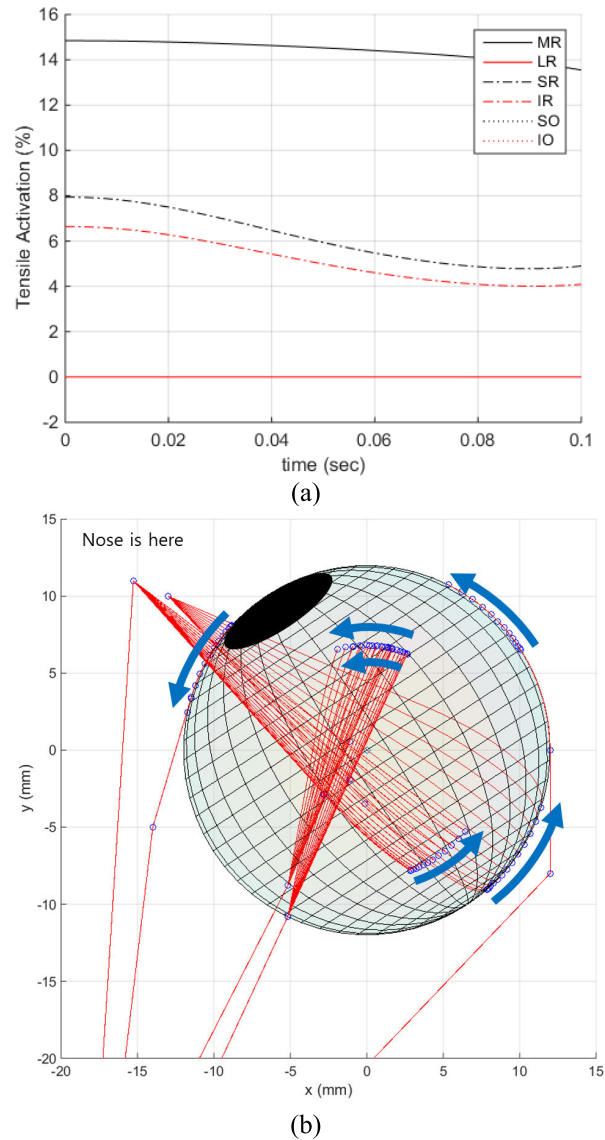


FIGURE 7. History of the muscle forces activation at Superior rectus (SR), Medial rectus (MR), and Inferior rectus (IR) to create the Adduction motion. (a) Muscles activation force to generate the Adduction motion. Three muscles are enough to generate the stable Adduction motion of the eyeball. The forces of SR, MR and IR are dominant while other muscle forces are negligible (b) The incremental changes in muscles length during dynamic motion of eyeball (top view).

disturbance given to this direction. The same phenomenon is observed in other muscle group to create any specific primitive motion of the eyeball. On the other hand, in the third plot, the torque value is $T_z = 4.8 \times 10^4 \text{ mg.mm}^2 / \text{sec}^2$, which actually contribute to Adduction motion. The same phenomenon is observed for Abduction motion. Where the summation of moment component about x and y-axis are zeros however, summation of moment components about z-axis given negative values which contribute in abduction motion. Finally, it is summarized that three muscles collaborate to create Adduction motion (i.e., counterclockwise rotation about z-axis).

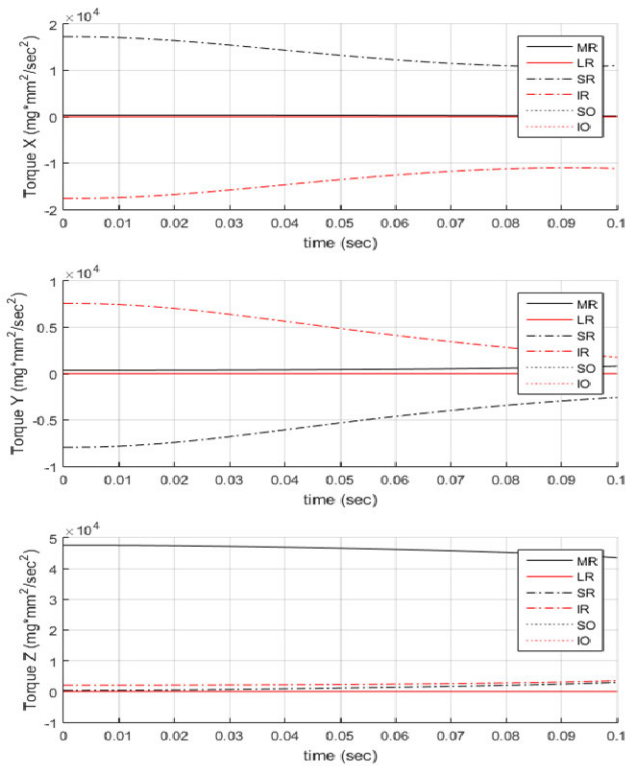


FIGURE 8. History of torque experienced by the eyeball due to muscles activation force of Superior rectus, Medial rectus, and Inferior rectus; x, y, and z-component of (11) in order. In first two plots, the summations of torque components are zero. Which shows that antagonistic internal loading to avoid any rotation about x- and y-axis. The torque due to Medial rectus (MR) in third plot contribute in Adduction motion.

Next, Depression motion (clockwise rotation about the x-axis) is analyzed. According to previous clinical research as given in Table 1, Superior oblique (SO) and Inferior rectus (IR) contribute to this motion. The muscle forces for Superior oblique and Inferior rectus are calculated based on the prozed model as given in Eq. (9), which contribute to create the Depression motion. Fig. 9(a) show the forces history for Depression motion. It can be seen that, muscles forces of SO and IR muscle are dominant while the other muscle forces are negligible. These muscle forces have positive values. By using these calculated muscle forces, the eyeball motion is simulated by performing the numerical integration of dynamic model as given in Eq. (2). Fig. 9(b) demonstrates the result of the dynamic simulation. Which denote the incremental changes in muscle lengths during the Depression motion. The figure shows the side view of the eyeball and trajectory of two muscles are shown as red lines.

Similar to Adduction motion, the internal loading affect is also analyzed for Depression motion. Similar to Eq. (11), the resulting torque vector projected to the operational space of the eyeball for depression motion is expressed in the following form:

$$\vec{T} = \vec{r}_{IR} \times \vec{F}_{IR} + \vec{r}_{SO} \times \vec{F}_{SO} = \begin{bmatrix} \{a_{IR}\}_x + \{b_{SO}\}_x \\ \{a_{IR}\}_y + \{b_{SO}\}_y \\ \{a_{IR}\}_z + \{b_{SO}\}_z \end{bmatrix}. \quad (12)$$

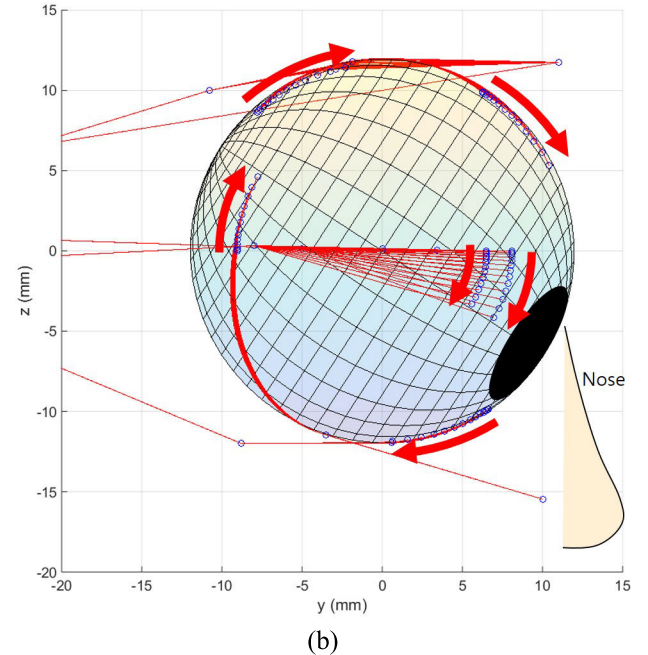
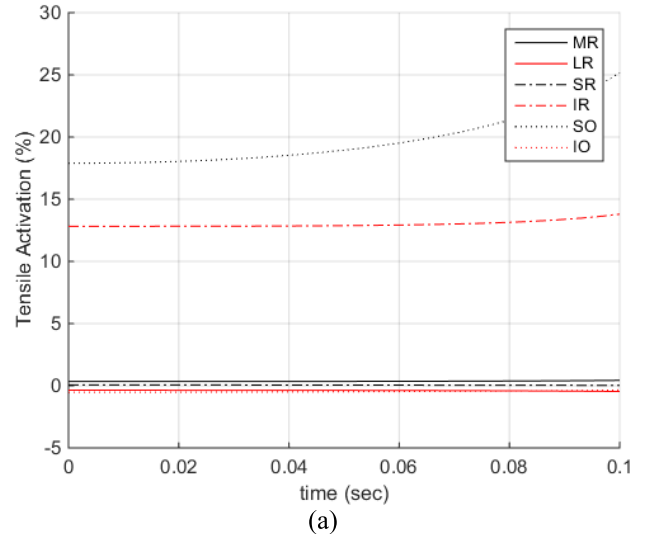


FIGURE 9. History of the muscle activation forces for Inferior rectus (IR) and Superior oblique (SO) to create the Depression motion. (a) Muscles activation force to create the Depression motion. The muscle force for IR and SO are dominant while the forces for other muscles are negligible (b) The incremental changes in muscle lengths during dynamic motion of eyeball (top view).

The first plot in Fig. 10 denotes the torque about x-axis. Two summation of moment components has negative sign. Physically, it implied that Superior oblique and Inferior rectus collaborate (load sharing) to create the Depression motion (clockwise rotation about the x-axis). Furthermore, the second plot denoting the y-directional torque has zero sum. Physically, it implied that they contribute to create antagonistic internal loading not to create any rotational motion about the y-axis. Lastly, the third plot denoting the z-directional torque has a constant minus sum. It implies that the eyeball is not completed balanced but rotates clock wisely by 0.86 degrees

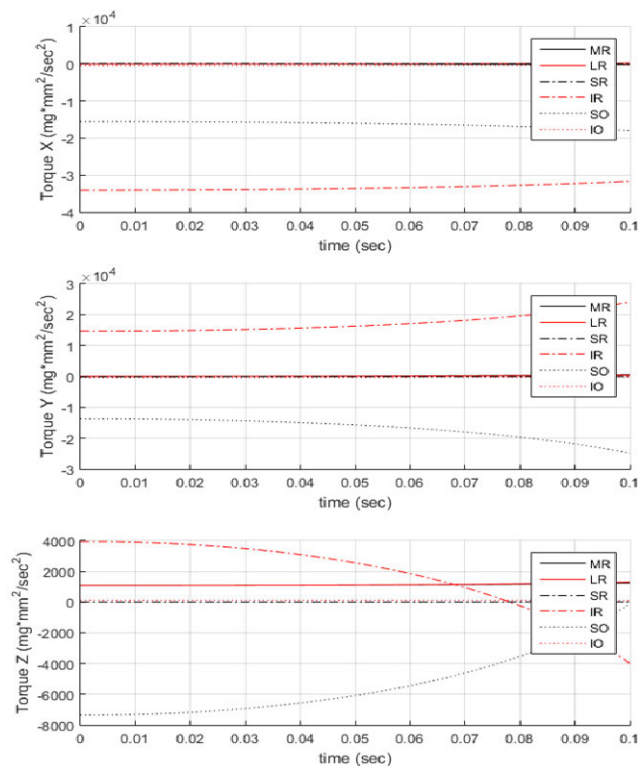
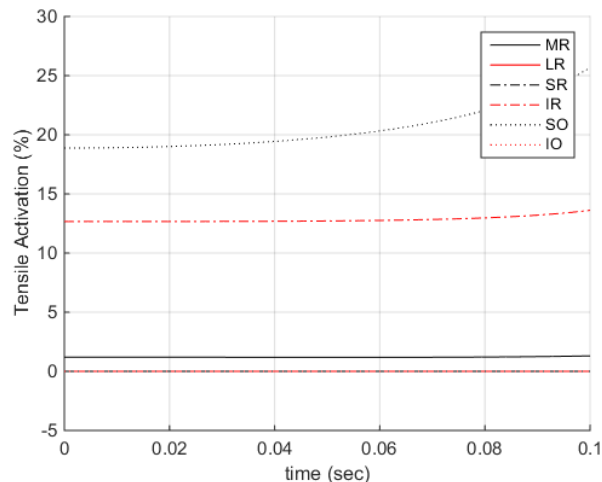


FIGURE 10. History of torque experienced by the eyeball due to muscles activation force of for Inferior rectus (IR) and Superior oblique (SO); x, y, and z-component of (12) in order. In first plot, the summation of components has negative sign that shows the depression motion of the eyeball. In the second plot, the summation of the torque components is zeros, which shows the antagonistic internal loading to avoid any rotation about y-axis. In last plot, the z-component has negative sum. The motion of the eyeball is not stable due to z-component.

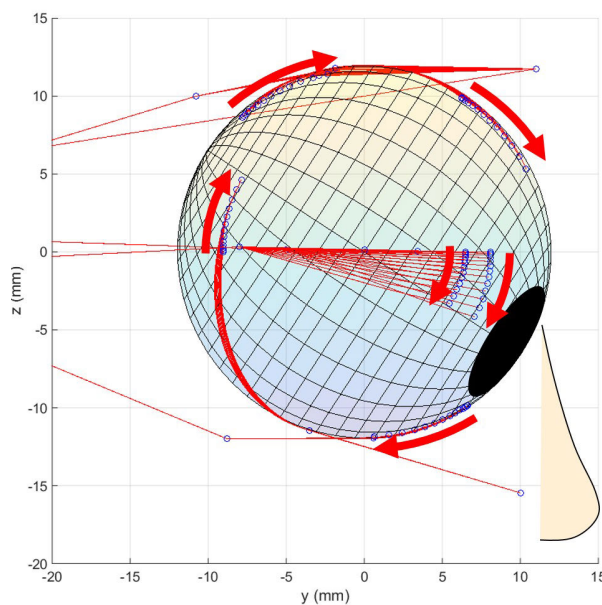
about the z-axis. Thus, it is noted that Depression is generated by using only two muscles while maintaining equilibrium about y-axis with slight offset angle about z-axis.

Similar phenomenon could be observed in motions of other extra-ocular muscles. When three muscles participate to motions such as Adduction and Abduction, their corresponding motion is successfully created, and internal loading does not create any motion in other directions. On the other hand, when only two muscles participate to motion such as Elevation and Depression, their corresponding motion is successfully created but some residual motion remains in one direction due to imperfect internal loading. It is presumed that such error may be due to incomplete analysis about the role of each extraocular muscles. Incorporating more muscles for Elevation and Depression like Adduction and Abduction motion would eliminate such motion residual problem.

We add one more extraocular muscle to create the Adduction motion. Medial rectus can be the candidate since it is analyzed to partially offset the residual of clockwise rotation of the eyeball about the z-axis. Finally, the proposed load distribution algorithm is applied by considering the three muscles. Through Fig. 11, it was confirmed that three muscle



(a)



(b)

FIGURE 11. History of the muscle activation forces for Inferior rectus, Superior oblique, and medial rectus to create the Depression motion. (a) Muscles activation force to generate the Depression motion. Three muscles are enough to generate the stable Depression motion of the eyeball. The forces of SO, MR and IR are dominant while other muscle forces are negligible (b) The incremental changes in muscle length during dynamic motion of eyeball (top view).

forces (e.g., Superior oblique, Inferior rectus, and Medial rectus) cooperate to create the Depression motion. It can be noted from Figs. 9(a) and 11(a) that the muscles forces are changed, which would generate extra antagonistic internal loading to keep eyeball balance in Depression motion.

Finally, the internal loading affect is analyzed by considering the three muscles for Depression motion. Similar to Eq. (11) and Eq. (12), when the muscle forces are mapped onto the center of the eyeball, the resulting torque vector projected to the operational space of the eyeball is expressed

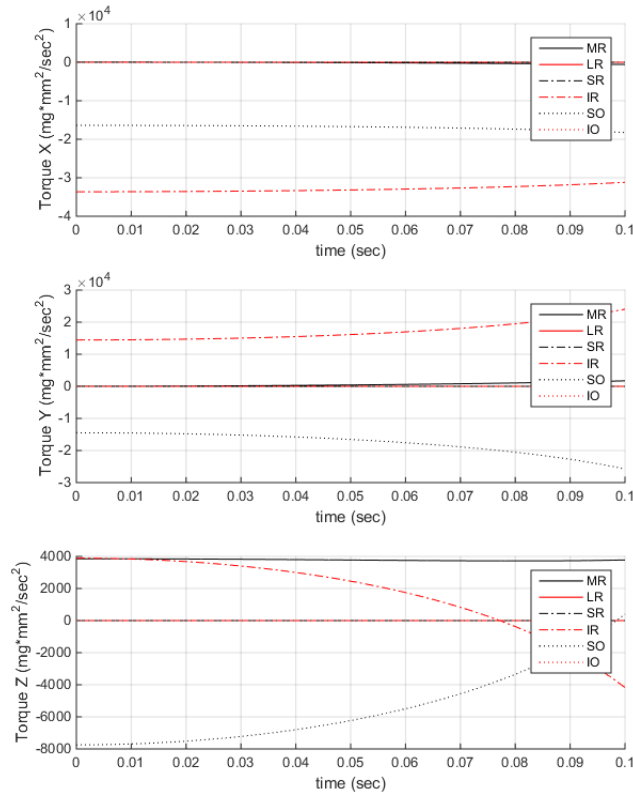


FIGURE 12. History of torque experienced by the eyeball due to muscles activation force of Inferior rectus, Superior oblique, and Medial rectus; x, y, and z-component of (11) in order. In first plot, the summation of components has negative sign that shows the depression motion of the eyeball. In the second and third plot, the summation of the torque components is zero, which shows the antagonistic internal loading to keep the eyeball stable during depression motion.

as the following form:

$$\begin{aligned}
 \vec{T} &= \vec{r}_{IR} \times \vec{F}_{IR} + \vec{r}_{SO} \times \vec{F}_{SO} + \vec{r}_{MR} \times \vec{F}_{MR} \\
 &= \begin{bmatrix} \{(a_{IR})_x + (b_{SO})_x + (c_{MR})_x\} \\ \{(c_{IR})_y + (b_{SO})_y + (c_{MR})_y\} \\ \{(c_{IR})_z + (b_{SO})_z + (c_{MR})_z\} \end{bmatrix} \\
 &= \begin{bmatrix} \text{moment sum @ x axis} \\ \text{moment sum @ y axis} \\ \text{moment sum @ z axis} \end{bmatrix}. \tag{13}
 \end{aligned}$$

In the first plot of Fig. 12, Superior oblique (SO) and Inferior rectus (IR) cooperate (load sharing) to create the Depression motion. In the second and third plots, summation of moment components is zero. Surprisingly, the internal loading in the other two directions (e.g., translation along the x-axis and rotation about the y-axis) is completely cancelled out without having any residual motion. It is confirmed that three muscle forces contribute to create antagonistic internal loading not to create any rotational motions about x- and y-axes. This was impossible using only two muscles. The same phenomenon is observed for Elevation motion. In order to eliminate any residual motion in Elevation, Lateral rectus (LR) should be added along with Superior oblique (SO) and Inferior rectus (IR). Where the summation of the

moment component about x-axis would have positive value that will contribute in Elevation motion. However, the summation about y-axis and z-axis would be zero that will help to balance eyeball in respective direction during depression motion. Similarly, Medial Rectus (MR) and Lateral rectus (LR) should be considered to create Intorsion and Extorsion, respectively as a third muscles, not to have any residual motion in other directions.

In summary, it is impossible to balance the eye while achieving main primitive motion with only two muscles. The eyeball should employ three independent extraocular muscles to create each primitive motion of the eyeball. Thus, based on the finding of this research, the first and second rows of Table 1 suggested by clinic people should be modified as mentioned in Table 3.

TABLE 3. Role of extraocular muscles (MR and LR).

Extra-ocular muscle	1 st effect	2 nd effect	3 rd effect
Medial Rectus (MR)	Adduction	<i>Depression</i>	<i>Intorsion</i>
Lateral Rectus (LR)	Abduction	<i>Elevation</i>	<i>Extorsion</i>
Superior Rectus (SR)	Elevation	Intorsion	Adduction
Inferior Rectus (IR)	Depression	Extorsion	Adduction
Superior Oblique (SO)	Intorsion	Depression	Abduction
Inferior Oblique (IO)	Extorsion	Elevation	Abduction

C. DISCUSSION

Inspired by inherent load sharing and antagonistic internal loading phenomenon of human eye, we proposed a load distribution algorithm to predict the muscles activation forces for specific motion. The focus of this research is to provide the solution by using valid assumptions. The assumptions made in this research are acceptable in robotics society, considering that this is a preliminary analysis of redundant actuation of human eyeball. We use the following assumptions. Detailed anatomy of the eye is rather complex. Whereas, in a simplified model, the human eyeball is roughly spherical, filled with a transparent gel-like substance called the vitreous humor [12]. We assumed eyeball model as solid sphere whose mass is uniformly distributed [3]. The gravity is ignored during dynamic simulation of the eyeball. The muscles are considered with zero width, as the mass and inertial effect of extraocular muscles are negligible compared to the mass of human eyeball. Currently, the effect of friction is not considered; however, it can be easily modeled in Eq. (2).

As shown in Fig. 3, misalignment between muscle axis and anatomical axis is inevitable because of anatomical structure of the human eyeball. However, this study discovered that such anatomical arrangement, on the other hand, is helpful to create internal loading as well as motion using minimum number of muscles. This is truly beneficial, because more muscles should be used to create motion and internal loading

simultaneously if muscle axis and eyeball axis are parallel. In previous study by FE modeling, the eye movements were produced by changing temperature and ignoring and including the parts' inertias, respectively [3], [9]. However, insight detail of muscle activation, considering the inherent load sharing and antagonistic internal loading phenomenon, is not explained in detail.

Mathematical modeling of the eyeball driven by six extraocular muscles enable us to estimate the required muscles forces to create the corresponding eyeball motions. In fact, out of six eye muscles, three were used to create the motion and the other three were used to select the muscles being used for a specific primitive motion. Therefore, there is no more remaining redundancy in muscle.

In addition, such mathematical model is useful to analyze the role of each muscle contributed to each primitive motion of the eyeball. It is found that all primitive motions require three extraocular muscles, which is different from the previous report [21], saying that Depression and Elevation are contributed by only two muscle groups. At least three or more than three muscles will be involved during generation of mixed motion, which are combination of roll, pitch and yaw motion.

The analytical method to estimate the extra-ocular muscle forces can be beneficially applied to analyze the motion characteristics of Vertigo and some disease due to ocular misalignment [41]. Some noise study to validate the suggested mathematical model and search for new finding should be further investigated in the future.

V. CONCLUSION

In this work, we analyzed the eyeball mechanics by explaining that how the human's eyeball is operated using six extraocular muscles for six primitive motions. The main contribution of this work is to analyze the force redundant system by developing a new mathematical model. Firstly, this work is provision of analytical motion model of eyeball in terms of extraocular muscle dynamics. It is analyzed that inherent anatomical arrangement of extraocular muscles is meaningful in the sense that using minimum number of muscles, both motion and internal loading can be achieved. Secondly, a novel load distribution algorithm is developed to explain the inherent muscle activation of human eyeball for each primitive motion in an analytical manner. Finally, through the analysis of the muscle force equations and dynamic simulations of the eyeball motion, it is analyzed that the extraocular muscles are arranged geometrically effective not only to generate primitive motion but also to increase the internal loading to resist external disturbance exerted in other motion directions, using the minimal number of muscles. Moreover, it is also found that at least three independent muscle should be activated to keep eyeball balance for each primitive motion.

The analysis of eye mechanics based on proposed novel load distribution algorithm and the understanding of more accurate physical role of extraocular muscle would certainly

help in development of more efficient vision system with superior performance close to the one of the human eyes.

APPENDIX

See Table 4.

TABLE 4. Constraints of muscle groups.

Primitive motion	[A]	$\vec{\alpha}$
Elevation	$[A] = \begin{bmatrix} 0 & 1 & 0 & 0 & 0 & 0 \\ 0 & 0 & 0 & 1 & 0 & 0 \\ 0 & 0 & 0 & 0 & 1 & 0 \end{bmatrix}$	$\vec{\alpha} = \begin{pmatrix} 0 \\ 0 \\ 0 \end{pmatrix}$
Depression	$[A] = \begin{bmatrix} 1 & 0 & 0 & 0 & 0 & 0 \\ 0 & 0 & 1 & 0 & 0 & 0 \\ 0 & 0 & 0 & 0 & 0 & 1 \end{bmatrix}$	$\vec{\alpha} = \begin{pmatrix} 0 \\ 0 \\ 0 \end{pmatrix}$
Adduction	$[A] = \begin{bmatrix} 0 & 1 & 0 & 0 & 0 & 0 \\ 0 & 0 & 1 & 0 & 0 & 0 \\ 0 & 0 & 0 & 0 & 0 & 1 \end{bmatrix}$	$\vec{\alpha} = \begin{pmatrix} 0 \\ 0 \\ 0 \end{pmatrix}$
Abduction	$[A] = \begin{bmatrix} 1 & 0 & 0 & 0 & 0 & 0 \\ 0 & 0 & 0 & 1 & 0 & 0 \\ 0 & 0 & 0 & 0 & 1 & 0 \end{bmatrix}$	$\vec{\alpha} = \begin{pmatrix} 0 \\ 0 \\ 0 \end{pmatrix}$
Extorsion	$[A] = \begin{bmatrix} 1 & 0 & 0 & 0 & 0 & 0 \\ 0 & 1 & 0 & 0 & 0 & 0 \\ 0 & 0 & 1 & 0 & 0 & 0 \end{bmatrix}$	$\vec{\alpha} = \begin{pmatrix} 0 \\ 0 \\ 0 \end{pmatrix}$
Intorsion	$[A] = \begin{bmatrix} 0 & 0 & 0 & 1 & 0 & 0 \\ 0 & 0 & 0 & 0 & 1 & 0 \\ 0 & 0 & 0 & 0 & 0 & 1 \end{bmatrix}$	$\vec{\alpha} = \begin{pmatrix} 0 \\ 0 \\ 0 \end{pmatrix}$

REFERENCES

- [1] G. Westheimer and S. P. McKee, "Visual acuity in the presence of retinal-image motion," *J. Opt. Soc. Amer.*, vol. 65, no. 7, p. 847, Jul. 1975.
- [2] N. J. Hall, Y. Yang, and S. G. Lisberger, "Multiple components in direction learning in smooth pursuit eye movements of monkeys," *J. Neurophysiol.*, vol. 120, no. 4, pp. 2020–2035, Oct. 2018.
- [3] S. Schutte, S. P. W. van den Bedem, F. van Keulen, F. C. T. van der Helm, and H. J. Simonsz, "A finite-element analysis model of orbital biomechanics," *Vis. Res.*, vol. 46, no. 11, pp. 1724–1731, May 2006.
- [4] D. A. Robinson, "A quantitative analysis of extraocular muscle cooperation and squint," *Investigative Ophthalmol. Vis. Sci.*, vol. 14, no. 11, pp. 801–825, 1975.
- [5] J. M. Miller and D. A. Robinson, "A model of the mechanics of binocular alignment," *Comput. Biomed. Res.*, vol. 17, no. 5, pp. 436–470, Oct. 1984.
- [6] J. M. Miller, "Functional anatomy of normal human rectus muscles," *Vis. Res.*, vol. 29, no. 2, pp. 223–240, Jan. 1989.
- [7] T. Haslwanter, "Mathematics of three-dimensional eye rotations," *Vis. Res.*, vol. 35, no. 12, pp. 1727–1739, Jun. 1995.
- [8] E. Bayro-Corrochano, "Modeling the 3D kinematics of the eye in the geometric algebra framework," *Pattern Recognit.*, vol. 36, no. 12, pp. 2993–3012, Dec. 2003.
- [9] A. Karami, M. Eghtesad, and S. A. Haghpanah, "Prediction of muscle activation for an eye movement with finite element modeling," *Comput. Biol. Med.*, vol. 89, pp. 368–378, Oct. 2017.
- [10] O. V. Komogortsev and U. K. S. Jayarathna, "2D oculomotor plant mathematical model for eye movement simulation," in *Proc. 8th IEEE Int. Conf. Bioinf. BioEng.*, Oct. 2008, pp. 1–8.

- [11] H. Guo, Z. Gao, and W. Chen, "Contractile force of human extraocular muscle: A theoretical analysis," *Appl. Bionics Biomech.*, vol. 2016, pp. 1–8, Mar. 2016.
- [12] Y. Zhang, J. Liu, K. Qi, and Z. Liu, "Modeling, design and analysis of a biomimetic eyeball-like robot with accommodation mechanism," in *Proc. IEEE Int. Conf. Robot. Biomimetics (ROBIO)*, Dec. 2013, pp. 861–866.
- [13] X.-Y. Wang, Y. Zhang, X.-J. Fu, and G.-S. Xiang, "Design and kinematic analysis of a novel humanoid robot eye using pneumatic artificial muscles," *J. Bionic Eng.*, vol. 5, no. 3, pp. 264–270, Sep. 2008.
- [14] S. Schulz, S. M. Z. Borgsen, and S. Wachsmuth, "See and be seen—Rapid and likeable high-definition camera-eye for anthropomorphic robots," in *Proc. Int. Conf. Robot. Automat. (ICRA)*, May 2019, pp. 2524–2530.
- [15] A. D. Polpitiya, W. P. Dayawansa, C. F. Martin, and B. K. Ghosh, "Geometry and control of human eye movements," *IEEE Trans. Autom. Control*, vol. 52, no. 2, pp. 170–180, Feb. 2007.
- [16] C. A. T. Suárez, "Isodeformation curves of the extraocular muscles from the inverse kinematics of a cable-driven parallel kinematics mechanism model of the eye," *Sci. Tech.*, vol. 23, no. 4, pp. 606–612, 2019.
- [17] G. Cannata and M. Maggiali, "Models for the design of bioinspired robot eyes," *IEEE Trans. Robot.*, vol. 24, no. 1, pp. 27–44, Feb. 2008.
- [18] L. Luo, N. Koyama, K. Ogawa, and H. Ishiguro, "Robotic eyes that express personality," *Adv. Robot.*, vol. 33, nos. 7–8, pp. 350–359, Apr. 2019.
- [19] M. M. Khan and C. Chen, "Design of a single cam single actuator multi-loop eyeball mechanism," in *Proc. IEEE-RAS 18th Int. Conf. Hum. Robots (Humanoids)*, Nov. 2018, pp. 1143–1149.
- [20] K. W. Wright, *Anatomy and Physiology of Eye Movements*. New York, NY, USA: Springer, 2003.
- [21] M. Buchberger, "Biomechanical modelling of the human eye," Ph.D. dissertation, Johannes Kepler Univ. Linz, Linz, Austria, 2004.
- [22] A. Priamnikov, M. Fronius, B. Shi, and J. Triesch, "OpenEyeSim: A biomechanical model for simulation of closed-loop visual perception," *J. Vis.*, vol. 16, no. 15, p. 25, Dec. 2016.
- [23] J. Arata, H. Kondo, N. Ikedo, and H. Fujimoto, "Haptic device using a newly developed redundant parallel mechanism," *IEEE Trans. Robot.*, vol. 27, no. 2, pp. 201–214, Apr. 2011.
- [24] Q. Li, N. Zhang, and F. Wang, "New indices for optimal design of redundantly actuated parallel manipulators," *J. Mech. Robot.*, vol. 9, no. 1, pp. 011007-1–011007-10, Feb. 2017.
- [25] D. Liang, Y. Song, T. Sun, and G. Dong, "Optimum design of a novel redundantly actuated parallel manipulator with multiple actuation modes for high kinematic and dynamic performance," *Nonlinear Dyn.*, vol. 83, nos. 1–2, pp. 631–658, Jan. 2016.
- [26] A. Müller, "Internal preload control of redundantly actuated parallel manipulators—Its application to backlash avoiding control," *IEEE Trans. Robot.*, vol. 21, no. 4, pp. 668–677, Aug. 2005.
- [27] B.-J. Yi and W. K. Kim, "The kinematics for redundantly actuated omnidirectional mobile robots," *J. Robot. Syst.*, vol. 19, no. 6, pp. 255–267, Jun. 2002.
- [28] B.-J. Yi, S.-R. Oh, and I. H. Suh, "A five-bar finger mechanism involving redundant actuators: Analysis and its applications," *IEEE Trans. Robot. Autom.*, vol. 15, no. 6, pp. 1001–1010, Dec. 1999.
- [29] J. Kim, F. C. Park, S. J. Ryu, J. Kim, J. C. Hwang, C. Park, and C. C. Iurascu, "Design and analysis of a redundantly actuated parallel mechanism for rapid machining," *IEEE Trans. Robot. Autom.*, vol. 17, no. 4, pp. 423–434, Aug. 2001.
- [30] S. H. Woo, S. M. Kim, M. G. Kim, B.-J. Yi, and W. Kim, "Torque-balancing algorithm for the redundantly actuated parallel mechanism," *Mechatronics*, vol. 42, pp. 41–51, Apr. 2017.
- [31] V. Salvucci, Y. Kimura, S. Oh, T. Koseki, and Y. Hori, "Comparing approaches for actuator redundancy resolution in biarticularly-actuated robot arms," *IEEE/ASME Trans. Mechatronics*, vol. 19, no. 2, pp. 765–776, Apr. 2014.
- [32] C. Gosselin and M. Grenier, "On the determination of the force distribution in overconstrained cable-driven parallel mechanisms," *Meccanica*, vol. 46, no. 1, pp. 3–15, 2011.
- [33] P. H. Borgstrom, B. L. Jordan, G. S. Sukhatme, M. A. Batalin, and W. J. Kaiser, "Rapid computation of optimally safe tension distributions for parallel cable-driven robots," *IEEE Trans. Robot.*, vol. 25, no. 6, pp. 1271–1281, Dec. 2009.
- [34] R. Verhoeven, "Analysis of the workspace of tendon-based Stewart platforms," Ph.D. dissertation, Dept. Mech. Eng., Univ. Duisburg-Essen, Duisburg, Germany, 2004.
- [35] S.-R. Oh and S. K. Agrawal, "Cable suspended planar robots with redundant cables: Controllers with positive tensions," *IEEE Trans. Robot.*, vol. 21, no. 3, pp. 457–465, Jun. 2005.
- [36] J. Lamaury and M. A. Gouttefarde, "Tension distribution method with improved computational efficiency," in *Cable-Driven Parallel Robots (Mechanisms and Machine Science)*, vol. 12. Berlin, Germany: Springer, 2013, pp. 71–85.
- [37] A. V. Hill, "The heat of shortening and the dynamic constants of muscle," *Proc. Roy. Soc. London B, Biol. Sci.*, vol. 126, no. 843, pp. 136–195, 1938.
- [38] S. R. Hamner, A. Seth, and S. L. Delp, "Muscle contributions to propulsion and support during running," *J. Biomech.*, vol. 43, no. 14, pp. 2709–2716, Oct. 2010.
- [39] E. Sifakis, I. Neverov, and R. Fedkiw, "Automatic determination of facial muscle activations from sparse motion capture marker data," *ACM Trans. Graph.*, vol. 24, no. 3, pp. 417–425, 2005.
- [40] I. Stavness, J. E. Lloyd, and S. Fels, "Automatic prediction of tongue muscle activations using a finite element model," *J. Biomech.*, vol. 45, no. 16, pp. 2841–2848, Nov. 2012.
- [41] Q. Wei, "Biomechanical modeling and simulation of human eye movement," Ph.D. dissertation, Dept. Comput. Sci., State Univ. New Jersey, New York, NY, USA, 2010.



control, exoskeleton hand motion capture, and virtual reality.

JUNGKYU KIM received the B.S. degree in information and communication engineering from Hansung University, Seoul, South Korea, in 2015, and the M.S. degree in electronic systems engineering from Hanyang University, South Korea, in 2018. He is currently a Researcher with the Center of Human-centered Interaction for Coexistence, Korea Institute of Science and Technology. His research interests include bio-inspired manipulators, object tracking, vision-based robot



motion capture, and virtual reality.

ABID IMRAN received the B.S. degree in mechatronics and control engineering from the University of Engineering and Technology, Lahore, Pakistan, in 2011, and the M.S. leading to Ph.D. degree in electronic systems engineering from Hanyang University, South Korea, in 2019. From March 2019 to August 2019, he was a Postdoctoral Fellow with the Research Institute of Engineering and Technology, Hanyang University. He is currently an Assistant Professor with the Faculty of Mechanical Engineering, Ghulam Ishaq Khan Institute of Engineering Sciences and Technology (GIKI). His research interests include motion optimization, biomimetics, bio-inspired manipulators, and impact mechanics.



motion capture, and virtual reality.

BYUNG-JU YI (Member, IEEE) received the B.S. degree from Hanyang University, Seoul, South Korea, in 1984, and the M.S. and Ph.D. degrees from The University of Texas at Austin, Austin, TX, USA, in 1986 and 1991, respectively, all in mechanical engineering.

From January 1991 to August 1992, he was a Postdoctoral Fellow with the Robotics Group, The University of Texas at Austin. From September 1992 to February 1995, he was an Assistant Professor with the Department of Mechanical and Control Engineering, Korea Institute of Technology and Education, Cheonan, Chungnam, South Korea. In March 1995, he joined the Department of Control and Instrumentation Engineering, Hanyang University. He was a Visiting Professor with Johns Hopkins University, Baltimore, MA, USA, in 2004. He was a JSPS Fellow with Kyushu University, Japan, in 2011. He is currently a Professor with the Department of Electronic Systems Engineering, Hanyang University. His research interests include general robot mechanics with application to surgical robotic systems (ENT, neurosurgical, and needle insertion areas), deep learning-based robotic manipulation, and ubiquitous sensor network-based robotics. He is a member of the IEEE Robotics and Automation Society. From 2005 to 2008, he was an Associate Editor of the IEEE TRANSACTIONS ON ROBOTICS. He is currently the President-Elect of the Korean Robotics Society and the Korean Society of Medical Robotics.

• • •